

Modeling and Analysis of Flexible Foot Vibration of Multi-Foot Bionic Robot

Lei Zhang

Department of Automation
Ocean University of China
Qingdao, 266100, China
zhanglei1107@ouc.edu.cn

Ang Li

Department of Automation
Ocean University of China
Qingdao, 266100, China
laqe9418@126.com

Zenghui Gao

Department of Automation
Ocean University of China
Qingdao, 266100, China
gzh951367198@163.com

Abstract—In order to solve the problems of large impact force and poor adaptability to complex surface of foot robot in motion, a flexible foot end with two degrees of freedom is proposed and designed. However, the structural characteristics of the foot end and the flexibility of the material lead to a phenomenon in the movement of the robot with this foot end. In order to solve this vibration phenomenon, a two-degree-of-freedom mathematical model of foot vibration is established by analyzing the foot structure and material characteristics. The vibration characteristics of the foot end are analyzed by simulation experiments, and the vibration characteristics of the foot end of different structures are compared. It is verified that the vibration characteristics of the model established in this paper are consistent with the vibration characteristics of the foot end measured by the actual robot experimental platform, which provides an accurate model basis for the next step to achieve vibration suppression through various control methods and motion strategies.

Index Terms—Multi-footed robot; Flexible foot; Vibration model;

I. INTRODUCTION

Multi-legged robots are widely used in complex working environments due to their strong terrain adaptability and high flexibility [1][2]. However, there are many problems with these robots, such as large impact and limited operation space [3][4]. As the robot technology develops toward high speed and precision, the flexibility effect of components is becoming more and more obvious [5][6]. Research on flexible materials and flexible mechanisms is of great significance in improving the service life, compliance control, stability, and terrain adaptability of legged robots [7][8]. Flexible structures and materials have become an important direction for research on multi-legged robots.

In order to optimize the motion performance of the robot foot and reduce the impact between the foot and the ground, many research works have been conducted on flexible feet and flexible bionic joints. Kevin et al. designed and developed a hexapod robot leg structure that used the variable stiffness flexible leg "C-leg" to improve the robot's bounce ability.

*This work is partially supported by Supported by the National Natural Science Foundation of China (Grant 51279185)

In order to give full play to the motion performance of the foot-type robot and reduce the impact of the foot and the ground, a two-degree-of-freedom flexible foot-end element was designed and manufactured in our laboratory by using the results of bionics analysis in the previous work [9]. The foot end unit is composed of a compression spring structure and a flexible material sole, which greatly improves the foot end's absorbability to the ground impact. When the foot touches the ground, the flexible sole deforms to adapt to the complex terrain while reducing the impact force, and then the force is transmitted to the compression spring through the push-pull rod to achieve secondary absorption of the impact force. At the same time, in order to accurately measure the distribution of plantar force, we add force sensor to the foot structure, and complete the calibration of the sensor to realize the robot's foot force perception. And through the optimized design of the shape of the foot, the omnidirectional walking of the robot is realized. Because there are elastic structures and flexible materials in the designed foot, the robot will generate a certain degree of vibration in the process of motion [10]. This vibration phenomenon not only affects the stability of the robot, but also affects the posture of the robot during motion, thereby reducing the overall control accuracy of the robot.

In this paper, the two-degree-of-freedom foot-end vibration model based on the design of the foot end is established by analyzing the structural characteristics and material properties of the foot. The validity of the model is validated by the analysis of foot vibration characteristics through simulation experiments. At the same time, the influence of different flexible material parameters on foot vibration characteristics is compared and analyzed, which provides guidance for the selection of flexible material parameters under different conditions, and lays a model foundation for the design of subsequent control methods and motion strategies.

II. FLEXIBLE FOOT MECHANISM DESIGN

As shown in Fig.1, a two degree of freedom foot mechanism is designed by imitating the composition and movement characteristics of the insect's foot according to the principle

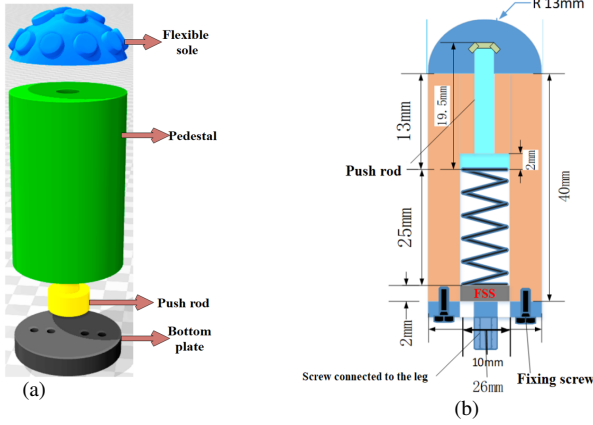


Fig. 1: Simplified model of foot mechanism:(a)Foot tip mechanical structure;(b)Foot tip sectional view

of bionics. The mechanism consists of six parts: flexible sole, base, push-pull rod, compression spring, pressure sensor and bottom plate. The base, sole and sole moulds are made with photosensitive resin by 3D printing technology, and the printing accuracy is 0.1 mm. The flexible sole of the robot is formed by injecting silicone HC9000 into the mould after printing and forming. The diameter of the foot end is 13mm, the height of the base is 40mm, and the overall mass is 45g.

The FSS pressure sensor is placed between the compression spring and the bottom plate. When the flexible material is deformed by force, the force is transmitted through the spring structure through the push-pull rod, and finally acts on the FSS pressure sensor. The pressure sensor can obtain the feedback information of the foot force in real time, which can effectively improve the environment adaptability and motion stability of the robot in complex terrain.

In order to study the cushioning characteristics of the designed foot structure, we designed a comparative motion experiment of robots with different foot structures. The hexapod robot in our laboratory is used as the test platform to carry the motion experiments on flexible and rigid foot ends respectively. The robot experiment platform with different foot ends is shown in Fig.2.

The hexapod robot is an all-aluminium frame with six legs symmetrically distributed and its foot ends are flexible; Joints are driven by digital servos; With K60 as the main control chip, it carries multi-channel sensors such as vision, infrared, attitude, ultrasonic and so on. The single leg movement time of the robot is set to 8 seconds. Voltage data are collected by DAQ-7606i data acquisition card. The acquisition accuracy is 0.152 mV. The robot moves in the form of three legs supporting each time, three legs swinging, and the foot end is in vertical contact with the ground. The voltage values of the rigid foot and the flexible foot during the walking process are separately recorded. By calibrating the sensor, the measured

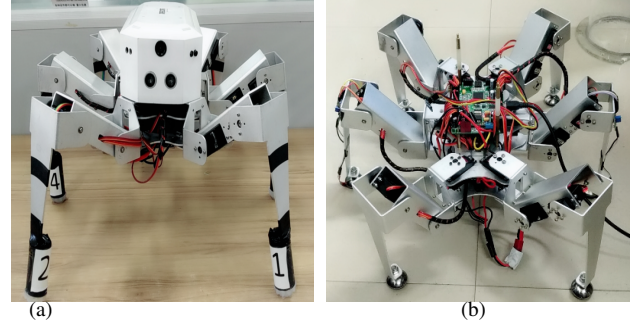


Fig. 2: Hexapod robot experiment platform:(a) Experimental platform with flexible foot ends; (b) Experimental platform with rigid foot ends

voltage value is converted into the foot end force, and two decimal places are reserved for the data processing.

The experimental results are shown in Fig.3.

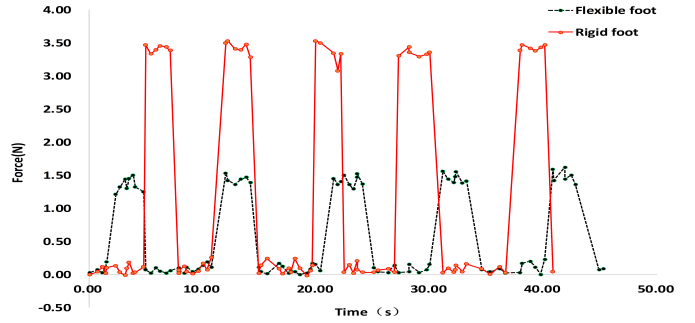


Fig. 3: Foot force change

As shown in Figure 3, the peak of the foot force of the robot with a flexible foot is significantly reduced compared to a rigid foot robot. In the course of robot walking, the average peak pressure of rigid foot is about 3.47N, while that of flexible foot is only 1.39N, which is 59% less than that of rigid foot. The experimental results show that the designed flexible foot has a significant effect on cushioning ground impact.

III. VIBRATION MODELING OF FLEXIBLE FOOT

The designed flexible foot structure contains flexible material and spring, which will produce large vibration in the process of robot motion [11]. During the movement of the robot, the vibration of the foot end will have a large impact on the motion characteristics of the robot, which will not only affect the stability of the robot, but also affect the posture of the robot, so that the robot can not fully achieve the desired control effect.

In order to better analyze the vibration characteristics of the foot, we designed the grounding experiment of the foot. The grounding experiment was also carried out on a hexapod

robot experimental platform with flexible foot ends. In order to better reflect the vibration characteristics of the robot's foot, the robot foot is repeatedly dropped from twice the height of the center of mass, that is, 27 cm from the ground and touched the ground vertically. During the experiment, the RFP patches pressure sensor is installed at the bottom of the robot's foot. The RFP sensor can measure the plantar pressure in the process of touching the ground and express the plantar force in the form of voltage. The plantar voltage of the foot is measured by the RFP pressure sensor installed on the sole of the foot, thereby obtaining the variation on the plantar force caused by the vibration of the foot in the process of touching the ground. By analyzing the variation of plantar voltage, we can obtain the vibration characteristics of the foot during the grounding process, and then establish the corresponding mathematical model. The variation on plantar voltage during the process of grounding is shown in Fig.4.

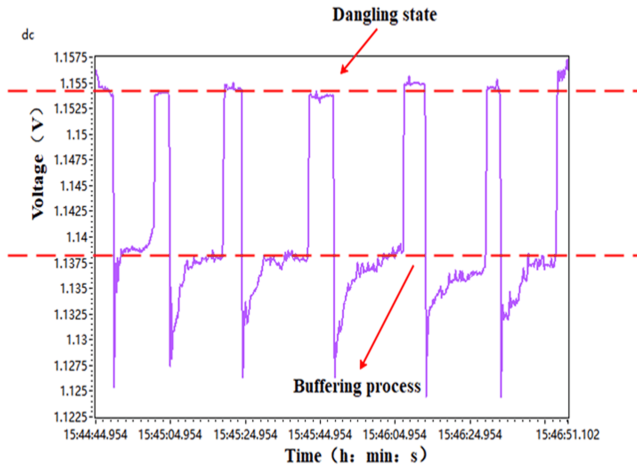


Fig. 4: Variation of plantar voltage

Fig.4 shows that the measured foot-sole voltage variations are similar to the vibration characteristics of a two-degree-of-freedom vibration system with damping. The actual vibration system in engineering is quite complex. When studying the vibration problem, it should be simplified according to the actual conditions and research purposes. Therefore, as shown in Fig. 5, a simplified two degree of freedom vibration model with linear damping is established based on the measured foot voltage variation characteristics and the designed foot end structure.

The flexible material at the foot end is regarded as a spring with linear damping [12], k_2 is the elastic coefficient, C is the linear damping coefficient, m_2 is the mass of push-pull rod, k_1 is the elastic coefficient of spring, and m_1 is the mass of the parts above the FSS sensor. Among them, $k_1=1.3N/mm$, $k_2=0.31N/mm$. When the thickness is 2.0 mm, the damping coefficient C is 0.11Nsec/mm, and

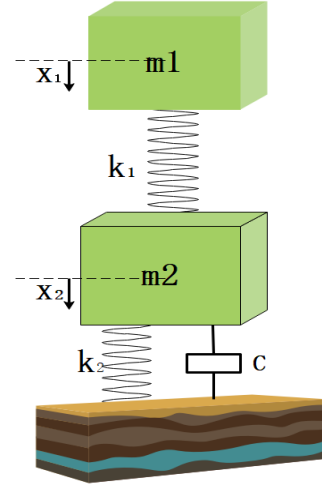


Fig. 5: Simplified foot vibration model

$m_2=45\text{ g}$. According to the weight component of each leg of the robot, $m_1=1.5\text{ kg}$ is taken.

Force analysis was performed on m_1 and m_2 in Fig. 5. Use x_1, x_2 to represent the displacement of m_1 and m_2 (take the center position). It can be seen that k_1 is the coupling spring of the two systems. Using Newton's second law, a differential equation of motion describing the system can be obtained:

$$\begin{cases} m_1\ddot{x}_1 + k_1(x_1 - x_2) = 0 \\ m_2\ddot{x}_2 + k_2x_2 + k_1(x_2 - x_1) + c\dot{x}_2 = 0 \end{cases} \quad (1)$$

Let:

$$\omega_{11}^2 = \frac{k_1}{m_1}, \omega_{21}^2 = \frac{k_1}{m_2}, \omega_{22}^2 = \frac{k_2}{m_2}, 2\varepsilon_{22} = \frac{c}{m_2} \quad (2)$$

ω_{11} is the natural frequency of M_1 relative to k_1 , ω_{21} is the natural frequency of M_2 relative to k_1 , and ω_{22} is the natural frequency of M_2 relative to k_2 . ε is the damping characteristic coefficient. At this time, the formula (1) becomes:

$$\begin{cases} \ddot{x}_1 + \omega_{11}^2x_1 - \omega_{21}^2x_2 = 0 \\ \ddot{x}_2 + (\omega_{21}^2 + \omega_{22}^2)x_2 - \omega_{21}^2x_1 + 2\varepsilon_{22}\dot{x}_2 = 0 \end{cases} \quad (3)$$

Express the solution to the equation as an exponential form:

$$\begin{cases} x_1 = A_1 \exp(\lambda t) \\ x_2 = A_2 \exp(\lambda t) \end{cases} \quad (4)$$

In the formula (4), A_1, A_2 represents the amplitude, and the formula (4) is substituted into the formula (1) to obtain:

$$\begin{cases} (\lambda^2 + \omega_{11}^2)A_1 - \omega_{21}^2A_2 = 0 \\ -\omega_{21}^2A_1 + (\lambda^2 + \omega_{22}^2 + \omega_{21}^2 + 2\varepsilon_{22}\lambda)A_2 = 0 \end{cases} \quad (5)$$

Since A_1 and A_2 cannot be zero at the same time, a pair of conjugates roots can be obtained from the above formula:

$$(\lambda^2 + \omega_{11}^2)(\lambda^2 + \omega_{22}^2 + \omega_{21}^2 + 2\varepsilon_{22}\lambda) - \omega_{21}^2\omega_{21}^2 = 0 \quad (6)$$

For the algebraic solution of equation (6), a pair of conjugate complex roots can be obtained.

$$\lambda = -\varepsilon \pm \omega i \quad (7)$$

The two roots of formula (7) are substituted into formula (4) respectively. After superposition, the general solution of the system can be obtained by Euler's formula:

$$x_1 = \exp(-\varepsilon t)[A_{1,1}\cos\omega t + A_{1,2}\sin\omega t] \quad (8)$$

M_1 is an undamped free vibration system, that is, the damping characteristic coefficient $\varepsilon_{11} = 0$, then the formula (8) can be expressed as:

$$x_1 = A_{1,1}\cos\omega t + A_{1,2}\sin\omega t \quad (9)$$

Where, $A_{1,1}, A_{1,2}$ are integral constants, which are determined by the initial conditions of vibration. For M_1 , when $t=0, x=x_0, dx/dt = v_0, A_{1,1} = x_0, A_{1,2} = v_0/\omega_{11}, \varphi_1$ is the initial phase.

Then the formula (9) becomes:

$$x_1 = x_0\cos\omega t + \frac{v_0}{\omega_{11}}\sin\omega t \quad (10)$$

Let $A_{1,1} = A_1\sin\varphi_1, A_{1,2} = A_1\cos\varphi_1, \omega = \omega_{11}$, the above formula can be further expressed as:

$$x_1 = A_1\sin(\omega_{11}t + \varphi_1) \quad (11)$$

In equation (11), A_1 represents the amplitude, $\omega_{11}t + \varphi_1$ represents the phase, and φ_1 represents the initial phase, where:

$$A_1 = \sqrt{A_{1,1}^2 + A_{1,2}^2}, \tan\varphi_1 = \frac{A_{1,1}}{A_{1,2}} \quad (12)$$

Also available for x_2 :

$$x_2 = \exp(-\varepsilon t)[A_{2,1}\cos\omega t + A_{2,2}\sin\omega t] \quad (13)$$

In equation (13), $A_{2,1}, A_{2,2}$ are integral constants, which are determined by the initial conditions of vibration. For M_2 , when $t = 0, x = x_0, dx/dt = v_0, A_{2,1} = x_0, A_{2,2} = (v_0 + \varepsilon x_0)/\omega_2, \varphi_2$ is the initial phase, $\omega_2 = \sqrt{\omega_{22}^2 - \varepsilon_{22}^2}$ is the natural frequency of the damped free vibration.

Substituting $\omega = \omega_2, \varepsilon = \varepsilon_{22}$ into equation (13):

$$x_2 = \exp(-\varepsilon_{22}t)(x_0\cos\omega_2t + \frac{v_0 + \varepsilon_{22}x_0}{\omega_2}\sin\omega_2t) \quad (14)$$

Let $A_{2,1} = A_2\sin\varphi_2, A_{2,2} = A_2\cos\varphi_2$, the above formula can be expressed as:

$$x_2 = A_2\exp(-\varepsilon_{22}t)\sin(\omega_2t + \varphi_2) \quad (15)$$

In formula (15), A_2 and φ_2 are integral constants determined by the initial conditions of vibration. For M_2 :

$$A_2 = \sqrt{x_0^2 + \frac{(v_0 + \varepsilon_{22}x_0)^2}{\omega_{22}^2 - \varepsilon_{22}^2}}, \tan\varphi_2 = \frac{x_0\sqrt{\omega_{22}^2 - \varepsilon_{22}^2}}{v_0 + \varepsilon_{22}x_0} \quad (16)$$

So the general form of the solution of equation (1) is:

$$\begin{cases} x_1 = A_1\sin(\omega_{11}t + \varphi_1) \\ x_2 = A_2\exp(-\varepsilon_{22}t)\sin(\omega_2t + \varphi_2) \end{cases} \quad (17)$$

From the formula (17), the vibration amplitude of the system can be obtained when the elastic parameters and damping coefficients are known. According to the actual engineering requirements, the appropriate design parameters are selected to meet the design requirements.

When the thickness of the flexible material is 2 mm, $c = 0.11 \text{ N} \cdot \text{sec}/\text{mm}$. When the robot is walking, the velocity component of the foot end is vertically downward $v_1(0)=v_2(0)=0.1 \text{ m/s}$. At the initial moment, $x_1(0)=0.05 \text{ m}$, $x_2(0)=0.01 \text{ m}$. Let $t=0.1 \text{ s}$, obtained by equations (2) and (12):

$$\omega_{11} = 0.93 \text{ rad/s}, A_{1,1} = 0.05 \text{ m}, A_{1,2} = 0.11 \text{ m}$$

$$A_1 = 0.12 \text{ m}, \tan\varphi_1 = 0.45, \varphi_1 = 0.42 \text{ rad}$$

Substitution (11) obtains:

$$x_1 = 0.06 \text{ m}$$

Then M_1 displacement is:

$$\Delta x_1 = x_1 - x_1(0) = 0.06 - 0.05 = 0.01 \text{ m} = 10 \text{ mm}$$

It can be obtained from formula (2) and formula (16):

$$\varepsilon_{22} = 1.22, \omega_{22}^2 = 6.89, \omega_2 = 2.32 \text{ rad}, A_{2,1} = 0.01 \text{ m}$$

$$A_{2,2} = 0.048 \text{ m}, A_2 = 0.048 \text{ m}, \varphi_2 = 0.20 \text{ rad}$$

Substitution (15) obtains:

$$x_2 = 0.014 \text{ m} = 14 \text{ mm}$$

Then the M_2 displacement is:

$$\Delta x_2 = x_2 - x_2(0) = 4 \text{ mm}$$

That is, when $c=0.11 \text{ N} \cdot \text{sec}/\text{mm}$ two degrees of freedom free vibration of the foot end, M_1 produces a displacement of 10 mm, and M_2 produces a displacement of 4 mm.

In the engineering practice, due to the existence of the natural frequency of the spring, the vibration phenomenon is inevitable when the elastic mechanism is added to the foot end. The more accurate vibration model is the basis for using the control method to reduce the vibration. The accuracy of the established model will be verified by simulation experiments. At the same time, comparative experiments are carried out to analyze the effects of different material characteristics on the vibration of the foot.

IV. SIMULATION ANALYSIS OF FOOT VIBRATION MODEL

A. Vibration model simulation of foot end mechanism with only flexible material

In order to study the influence of the vibration of the foot end on the motion, this paper analyzes the influence of the flexible material of the foot end and the spring mechanism on the motion of the robot through MATLAB/SIMULINK simulation.

The robot is set to move forward with the vertical velocity component of $0.1m/s$, and the initial position is set to $0.01m$. Set the mass of all parts above the robot's foot to M . There is only damping in the landing process.

When a flexible mechanism is added to the foot end, the flexible mechanism will deform when the robot lands on the foot. For the convenience of analysis, it is equivalent to an elastic mechanism with linear damping, and its elastic parameters are measured experimentally. Establish the model as shown in Fig.6.

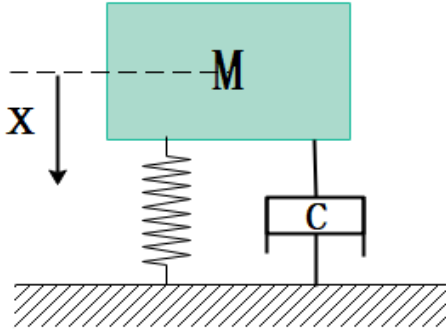


Fig. 6: Foot Vibration Model with Flexible Mechanisms

The elastic coefficient of the spring is $k_2=0.31N/mm$. The damping coefficient of composite flexible materials is related to thickness, as shown in Table 1. When the thickness is $2mm$, $c=0.11N \cdot sec/mm$. The damping of the composite is also affected by its internal molecules, and the typical value given is only a divisor, theoretically not exceeding the magnitude of the value. In order to analyze the effect of the thickness of the foot end on the vibration, the maximum diameter of the hemispherical foot is assumed to correspond to the maximum thickness. The maximum damping coefficient corresponding to its thickness is taken as input C , and the other parameters remain unchanged. The curve variation of displacement is analyzed.

TABLE I: Typical Value of Damping Coefficient

Thickness/ mm	2.0	5.0	7.0	9.0	11.0	13.0	20.0
Threshold Value	0.11	0.22	0.34	0.44	0.53	0.68	1.01

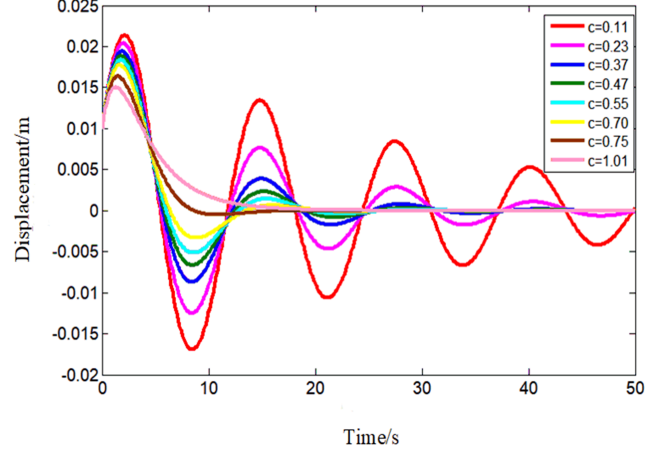


Fig. 7: Simulation results of different flexible parameters

Simlink is used to simulate the displacement. The sampling time is set to 50 by changing the C value. The displacement simulation results are shown in Fig. 7.

It can be seen from Fig. 7 that with the increase of C value, the buffer displacement gradually decreases and the attenuation speed gradually increases. In the actual movement of the robot, we hope that the foot end of the robot can generate a certain cushion displacement when landing, and can restore the movement stability in a short time. When the c value is equal to 0.7, that is, the yellow curve in the figure, the foot end is stabilized by two buffer displacements. When the c value is greater than 0.7, the foot end is stabilized after a buffering phase, and the corresponding displacement of the foot end is small. When the c value is less than 0.7, the foot end has to be buffered multiple times to achieve stability. Therefore, considering the buffer displacement and balance time, the damping coefficient of about 0.70 is the most satisfying requirement. The maximum diameter of the flexible material of the foot end is set to 13 mm, as shown by the yellow curve in the figure, and the buffer displacement at this time is about 7 mm.

B. Vibration Model Simulation of Two-degree-of-freedom Flexible Foot Mechanism

The designed foot-end mechanism has both flexible material and spring structure, which is equivalent to a two-degree-of-freedom system with linear damping. The vibration characteristics of the foot end were simulated by Simulink, and the simulation results are shown in Fig. 8. Initial velocity is constant, $v_1(0) = v_2(0) = 0.1m/s$, The remaining parameters remain unchanged. The landing moment of the foot flexible material is set as the initial time. $x_1(0) = 0.05m$, $x_2(0) = 0.01m$.

As shown in Figure 8, the displacement of the foot end reaches the maximum at the moment of contact during the

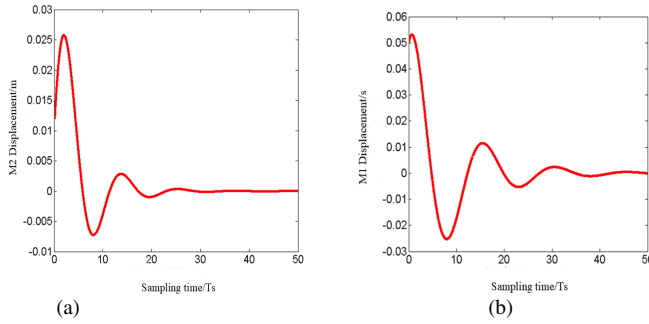


Fig. 8: Simulation results of flexible foot:(a)m1 displacement;(b)m2 displacement

vibration process, and the buffer is quickly generated. During the buffering process, the displacement gradually decreases and stabilizes after two buffering periods. During the whole vibration process, the peak time of the displacement and the buffer process of the vibration are consistent with the variation characteristics of the plantar voltage measured in the experiment. Therefore, the established model can better reflect the vibration characteristics of the actual foot end. The model foundation is made for the application of different control methods to reduce the vibration of the foot end.

V. CONCLUSION

Aiming at the vibration problem of a flexible foot with two degrees of freedom during the movement process, this paper establishes a two-degree-of-freedom foot-end vibration model by combining the characteristics of the plantar voltage and the structure of the foot end, and gives a more accurate mathematical description of the foot-end vibration characteristics. Through simulation experiments, the vibration characteristics of the model and the actual foot are compared, and the accuracy of the model is verified. By analyzing the foot ends with different material parameters, the influence of flexible material parameters on the vibration characteristics of the foot end was studied, and the mapping relationship between different material parameters and vibration characteristics was established, which provided a guide for selecting material parameters according to different conditions. The experimental and simulation verification shows that the vibration characteristics of the two-degree-of-freedom model established in this paper are consistent with the actual foot-end vibration characteristics measured on the robot experimental platform during the experiment. It can accurately reflect the actual foot vibration situation and provide an accurate model basis for the subsequent reduction of foot vibration through different control methods and motion strategies.

Subsequently, based on the vibration model established in this paper, the motion strategy and control method that fits the model will be adopted to achieve the purpose of reducing vibration and improving motion performance.

REFERENCES

- [1] Billah, M.M.; Ahmed, M.; Farhana, S. Walking hexapod robot in disaster recovery: Developing algorithm for terrain negotiation and navigation. *Proc. World Acad. Sci. Eng. Technol.* 2008, 42, 328-333.
- [2] Huang, Q.J.; Nonami, K. Humanitarian mine detecting six-legged walking robot and hybrid neuro walking control with position/force control. *Mechatronics* 2003, 13, 773-790.
- [3] Shi, Y.; Ding, G.; Zhang, M.; Zhang, X. Foot end trajectory with small oscillation generation method of the adjustable stiffness active flexible joint robot. In *Proceedings of the 2016 IEEE International Conference on Robotics and Biomimetics (ROBIO)*, Qingdao, China, 3-7 December 2016; pp. 455-460.
- [4] Low, K.H.; Yang, A. Design and foot contact of a leg mechanism with a flexible gear system. In *Proceedings of the 2003 IEEE International Conference on Robotics and Automation (Cat. No. 03CH37422)*, Taipei, Taiwan, 14-19 September 2003; Volume 1, pp. 324-329.
- [5] Fan Jihua, Z.G.; Hong, C. Dynamic analysis and simulation of robot considering joint flexibility. *Comput. Simul.* 2017, 8, 331-336.
- [6] Wen Li.; Wang Hesheng. Software robot research outlook: Structure, drive and control. *Robot* 2018, 40, 577-577.
- [7] Zhang, L.; Liu, X.; Guo, X. Development of Hexapod Robot with one passive joint on foot. In *Proceedings of the 2017 IEEE International Conference on Robotics and Biomimetics (ROBIO)*, Macau, China, 5-8 December 2017; pp. 1082-1087.
- [8] Yanlei, S.; Minglu, Z.; Xiaojun, Z. Design and analysis of four-legged mechanical legs with flexible joints. *J. Huazhong Univ. Sci. Technol. (Nat. Sci. Ed.)* 2017, 40, 3.
- [9] Lei Zhang, Xinzhi Liu, Ping Ren, Zenghui Gao and Ang Li. Design and Research of a Flexible Foot for a Multi-Foot Bionic Robot. *Appl. Sci.* 2019, 9(17), 3451.
- [10] WANG Zhenyu, YANG Fan, On, YUE Yi ngzhan, GE Wenjie. Motion Characteristics of Kangaroo Robot'S Flexible Foot Based on Uniform Flexible Beam Model during Touchdown Phase. *Robot* 2009, 31, 460-464.
- [11] Jianwen Luo, Yili Fu, Shuguo Wang, Mu Qiao. How do the Compliant Legs Affect Walking Stability? *International Conference on Robotics and Biomimetics (ROBIO)*, Macau, China, 5-8 December 2017; pp. 599-604.
- [12] Dunwen Wei; Tao Gao. Research of Power Modulation Characteristics of Elastic Actuators. *International Conference on Robotics and Biomimetics (ROBIO)*, Macau, China, 5-8 December 2017; pp. 276-281.